

Class I and Class II Subdivision of the 20-meter Geodesic Dome Behavior and Analysis using Breakdown Methods 1 and 2 for Various Dome Frequencies

Komal B. Lendave¹, P.V. Dhanshetti², Dr. S. S. Patil³

 Department of Civil Engineering, Walchand Institute of Technology, Solapur, Maharashtra, India, Email: komallendave23@gmail.com
Department of Civil Engineering, Walchand Institute of Technology, Solapur, Maharashtra, India, Email: pvdhanshetti@witsolapur.org
Department of Civil Engineering, Walchand Institute of Technology, Solapur, Maharashtra, India, Email: patilss1962@gmail.com

One of the most efficient buildings that can be built without interfering with columns to cover a larger area is a dome. These kinds of complicated structures depend heavily on modeling and analysis. There are many other kinds of domes, including ribbed, Schwedler, lamella, diametric, and geodesic ones, but the geodesic dome is one of the more effective ones. This investigation examines the separation of geodesic domes into Class I, concentrating on two different breakdown techniques, Methods 1 and 2. The structural strength and effective material usage of geodesic domes make them famous examples of architecture. This study examines the effects of various dome frequencies on the efficacy of certain subdivision techniques.

Keywords: Cadre Geo; Geodesic Dome; Class I Subdivision; Node and Beam Displacement; Spherical Structure.

I. INTRODUCTION

A geodesic dome is a unique kind of structure that resembles a large, spherical jungle gym. It has a spherical shape thanks to the assembly of numerous sturdy triangles. This spherical shape is highly robust and can be used for various things, such as a play area or a location to keep plants protected from the elements, just as how triangles are used in school. Networks of connected triangles, producing a spherical or partially spherical shape, make up a geodesic dome, a type of structural design. The architect and inventor R. Buckminster Fuller popularized the phrase in the middle of the 20th century. Not only are geodesic domes amazing to look at, but they are also quite robust and can be utilized for entertaining and practical purposes.

Scope of work

The following significant elements typically form the core of the scope of work for a class I subdivision utilizing breakdown procedures 1 and 2 for different dome frequencies:

- The goal of the subdivision and the precise dome frequencies that must be examined should be made clear in the project.
- Assemble all pertinent information, including topographic maps, geological details, and the results of any earlier surveys or investigations that may have been conducted in the area.
- Specify the dome's geometric characteristics, such as the dome's size, frequency, and type of geodesic structure.
- Analyze the dome's structure to determine its stability and load-carrying ability.
- Describe how the dome's design is optimum for various objectives, such as the building's architectural beauty, environmental sustainability, or practical utility.

II. METHODOLOGY

Certainly, here is a more detailed way to build a geodesic dome:

The base structure for this approach is the icosahedron, which is made up of 20 equilateral triangles. It may be used to create miniature domes and is reasonably easy to build. A class I geodesic dome is based on an icosahedron and simulates the sphere's shape using triangles of various sizes. There could be more or fewer triangles created depending on the frequency (number of subdivisions). The shape of higher-frequency domes is more spherical, but their construction and computations are more difficult. Several materials can be used to construct geodesic domes. I have chosen a circular hollow tube-size section for my research project. The endurance and strength of the dome can be greatly influenced by the material selection.

Using the CADRE Geo 7.0 software, the geodesic domes have been modeled. For analysis class I subdivision for breakdown methods 1 and 2, a 20-meter-diameter geodesic dome tuned to dome frequencies of 4v, 6v, 8v, 10v, and 12v is employed. STAAD PRO Connect Edition software received these domes for analysis. Steel is what's used to make the dome. The concept of fixed supports is used.

III. BREAKDOWN METHOD OF GEODESIC DOME

Geodesic domes are characterized based on the type of triangulation used for the primary polyhedron; these breakdown methods are defined as a geometric methodology for breaking down the geodesic face into smaller faces.

A. Method 1

It is performed by breaking down the flat triangular geodesic face sides into evenly spaced lengths (d, e, and f in the image below), then building the mesh over the triangle as shown, and then projecting the face onto the sphere. After projection, the lengths of the side segments (a, b, and c) will not be equal, nor will the spherical angles (A, B, C).

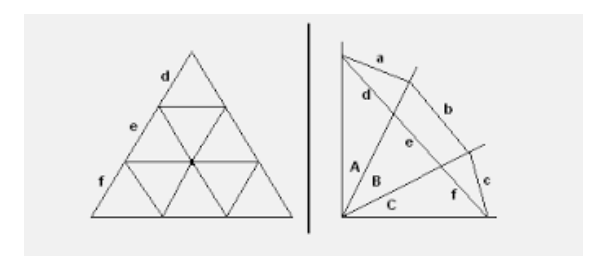


Figure 1 Breakdown method 1

B. Method 2

Method 2 was accomplished by dividing the edges of the geodesic face into equally spaced spherical angles so that d, e, and f on the flat triangle were not equal. When projected onto the sphere, the edges (a, b, c) and spherical angles (A, B, and C) will be equal.

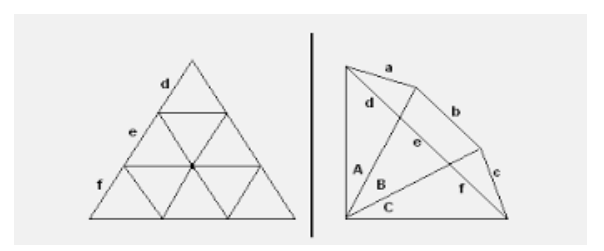


Figure 2 Breakdown 2

C. Method 3

Method III allows greater economy of fabrication at a slight cost in overall symmetry. The number of unique struts in a method III subdivision is equal to the frequency, i.e., 12 unique struts for a 12V sphere, 16 unique struts for a 16V sphere, 20unique struts for a 20V sphere, etc.

WARNING: Method III should only be used on perfect spheres. All economy of fabrication is lost when using ellipsoidal or egg type envelopes.

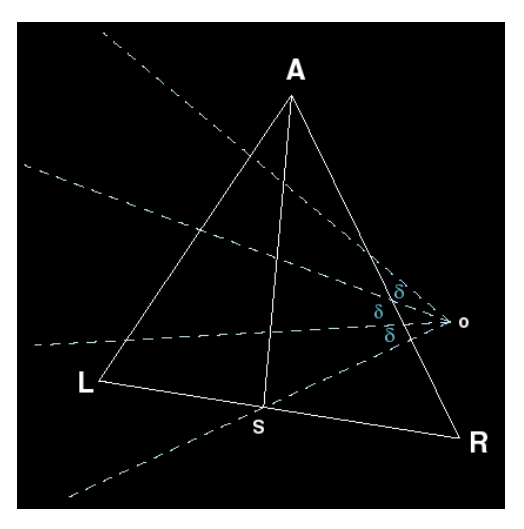


Figure 3 Breakdown method III

IV. PROBLEM FORMULATION

A. Validation of software based on existing literature

In this section, existing literature research are examined, and results are compared for validation purposes. The paper titled 'Comparative study for geodesic dome of class 1 subdivisions' is used for the existing literature study and validation, and it was published in the Journal of Emerging Technologies and Innovative Research (JETIR) in May 2016, Volume 3, Issue 5. This report presents a comparative examination of geodesic domes of class 1 subdivisions. Geodesic dome modeling is done using modeling software, while analytical design is done with STAAD-PRO software. The dome is simulated for various frequencies while keeping the span constant, and weights are compared. Paper titled 'Modelling & Validation of Single Layer Geodesic Dome with various Height to Span Ratios' is used for the current literature analysis and validation, as reported in the International Research Journal of Engineering and Technology (IRJET), May 2019, Volume 6, Issue 5. This study presents the modeling and validation of geodesic domes for various height to span ratios for class I subdivision and breakdown method I using SAP2000 and Staad Pro software. For validation, I used the same section material and analyzed and developed it in Staad Pro program.

B. Finding maximum axial force

Before going to start the work first figuring out where exactly maximum axial forces will be going to be act. Whether, it may act at top of dome or in middle or at bottom of dome. For figuring this I have considering, 10m radius of dome and 8v frequency dome for class 1 breakdown method 1. Geodesic domes were modelled using the CADRE Geo 7.0 program. These domes were imported on Staad Pro Connect Edition software for modelling and analysis purpose. The section size of strut as PIP1937L is considered for analysis. The material of dome is considered as steel. Supports are considered to be fixed.

After analysis, it is observed that maximum axial forces are acting in the bottom ring side of the structure & as we go toward the top of the structure the axial force is reducing. The % reduction for axial force from the bottom to the top of the structure is shown in Table 1.

Table 1: Percentage reduced axial force from bottom to top of structure

| | | \overline{c} | | | | | | | |
|--|-----|----------------|------|------|------|--------|-------|-------|----------------------|
| % Reduction of axial force 16.74 (TOP) | 3.6 | 18.7 | 10.5 | 15.7 | 10.9 | 4 3.11 | 11.87 | 14.88 | 8.41 (BOTTO M) |

C. Present Study

Geodesic dome of radius 20m & 4 frequency dome or "4v", 6v, 8v, 10v, 12v is being used for analysis for class I & class II subdivision for breakdown method I & method 2. The geodesic domes have been modeled with the help of the CADRE Geo 7.0 software. These domes were imported on Staad Pro Connect Edition software for modeling and analysis purposes. The material of the dome is considered steel. Supports are considered to be fixed.

Table 2: Material property for the member.

| Member material | Yield strength of steel (KN/mm ²) | Density (KN/m ³) | Poisson's ratio |
|-----------------|---|------------------------------|------------------------|
| Steel | 250×10^3 | 7833.409 | 300 x 10 ⁻³ |

It is determined after observation that the bottom rings have the greatest compressive axial force and can be clustered together. For example, the bottom four numbers of rings with the highest compressive axial force are labeled RING 1, RING 2, RING 3, and RING 4, correspondingly. From crown to ring, 4 people form a TOP-PENTAGON. The remaining bottom diagonal members between horizontal rings are referred to as BOTTOM-PENTAGON. After improving the model, the sectional characteristics of each member will differ. Members are grouped as shown below in Figure 1, Figure 2, and Figure 3. The grouping of members for different dome frequencies is shown in Table 4.

Table 3: Section property for the element

| Element type | External | periphery | Consistency | Area of a |
|--------------|----------|-----------|-------------|--------------------------|
| | (mm) | | (mm) | slice (cm ²) |
| PIP1524M | 152.4 | | 4.8 | 22.3 |
| PIP1651M | 165.1 | | 4.8 | 24.2 |
| PIP1397M | 139.7 | | 4.8 | 20.3 |
| PIP1937L | 193.7 | | 4.8 | 28.5 |
| PIP1270M | 127.0 | | 4.8 | 18.4 |
| PIP1270L | 127.0 | | 4.5 | 17.3 |

Table 4: Grouping of members

| 1 aut 4. 0100 | iping of incliders | |
|--|--------------------|--------------|
| Method | Ring | Section Size |
| 4v Class I and Class II Method 1 and 2 | Ring 1 | PIP1524M |
| | Ring 2 | PIP1651M |
| | Ring 3 | PIP1937M |
| | Ring 4 | PIP1397L |
| | Top pentagon | PIP1270M |
| | Bottom pentagon | PIP1270L |
| 6v Class I and Class II Method 1 and 2 | Ring 1 | PIP1524M |
| | Ring 2 | PIP1651M |

| | Ring 3 | PIP1937M |
|---|-----------------|----------|
| | Ring 4 | PIP1397L |
| | Top pentagon | PIP1270M |
| | Bottom pentagon | PIP1270L |
| 8v Class I and Class II Method 1 and 2 | Ring 1 | PIP1524M |
| | Ring 2 | PIP1524M |
| | Ring 3 | PIP1651M |
| | Ring 4 | PIP1937M |
| | Ring 5 | PIP1397L |
| | Top pentagon | PIP1270M |
| | Bottom pentagon | PIP1270L |
| 12v Class I and Class II Method 1 and 2 | Ring 1 | PIP1524M |
| | Ring 2 | PIP1524M |
| | Ring 3 | PIP1524M |
| | Ring 4 | PIP1524M |
| | Ring 5 | PIP1651M |
| | Ring 6 | PIP1937M |
| | Ring 7 | PIP1397L |
| | Top pentagon | PIP1270M |
| | Bottom pentagon | PIP1270L |
| 12v Class I and Class II Method 1 and 2 | Ring 1 | PIP1524M |
| | Ring 2 | PIP1524M |
| | Ring 3 | PIP1524M |
| | Ring 4 | PIP1651M |
| | Ring 5 | PIP1651M |
| | Ring 6 | PIP1937M |
| | Ring 7 | PIP1937M |
| | Ring 8 | PIP1397L |
| | Top pentagon | PIP1270M |
| | Bottom pentagon | PIP1270L |

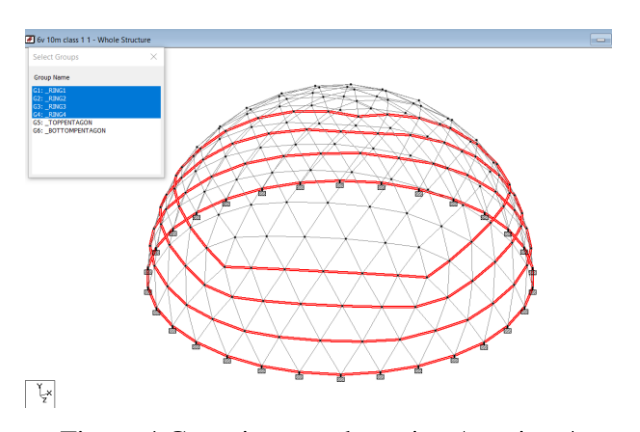


Figure 4 Grouping members ring 1 to ring 4

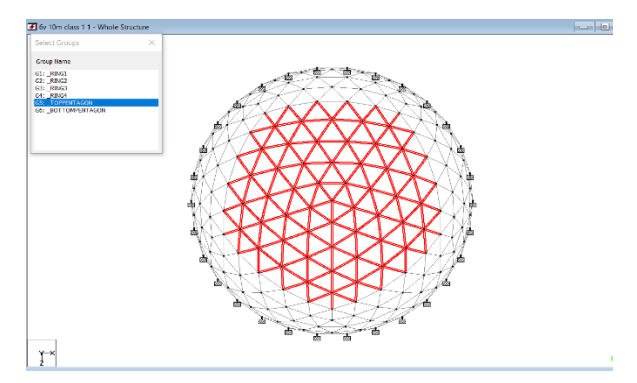


Figure 5 Grouping members at the top - pentagon.

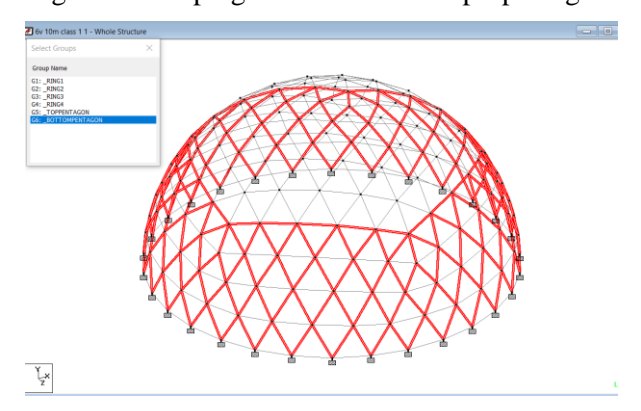


Figure 6 Grouping members at the bottom – pentagon

D. Analytical model of geodesic dome using CADRE Geo software

A plan for analyzing the model is built up. For breakdown technique 1, a 20-meter-wide geodesic dome model is created for class I and class II subdivisions.

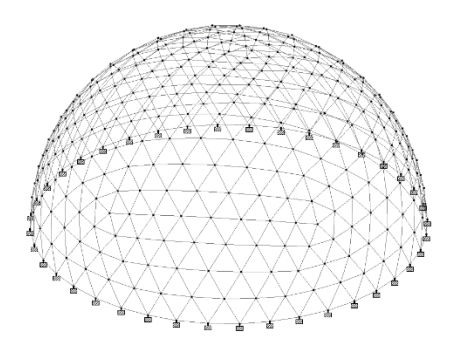


Figure 7 Class I method 1 8v dome

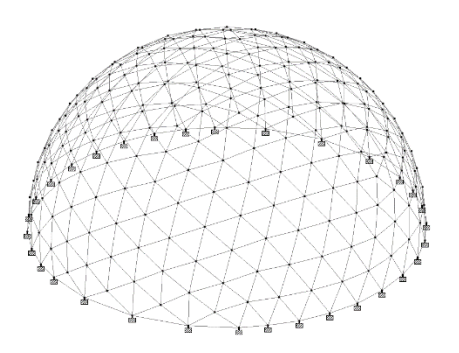


Figure 8 Class II method 1 8v dome

V. LOAD CASES

The analysis takes into account seismic, wind, dead, and living loads. Wind load is the dominant force in constructions with a dome form. IS 875 (part 3)-2015 is used to determine wind load. According to IS 800, load combinations are chosen.

A. Dead load (self-weight)

Steel members or struts, which are hollow steel pipe sections, make up the bulk of self-weight.

B. The live load

IS 875 (part 2) - 1987 is used to compute live load. 1.177 KN/m of uniform roof load is imposed as live load.

C. Wind load

IS 875 (part 3)-2015 was used to calculate the wind load on the structure. Take into account the ensuing factors.

Table 5: Wind - related parameters

| Basic wind speed | 50(m/sec) |
|--------------------------|-----------|
| Category | 1.00 |
| Risk coefficient (k1) | 1.08 |
| Landscape factor (k3) | 1.00 |
| Importance factor (k4) | 1.15 |
| Wind factor (Kd) | 1 (m/sec) |
| Average area factor (Ka) | 0.9 |
| Combination factor (Kc) | 0.9 |

Table 6: Intensity Vs. Height for staad pro

| | Terrain | Wind | $P(KN/m^2)$ | $0.7 * P_z$ | Pd max of |
|-------|------------|-----------------|-------------|-------------|-------------|
| Hight | &height | pressure | | (KN/m^2) | 0.7 * Pz & |
| підіі | multiplier | (Pz = | | | $P(KN/m^2)$ |
| | (k2) | $0.6 * V_Z^2$) | | | |
| 10 | 1.05 | 2001.0375 | 1.80093375 | 1.40072625 | 1.80093375 |
| 15 | 1.09 | 2156.4015 | 1.94076135 | 1.50948105 | 1.94076135 |
| 20 | 1.12 | 2276.736 | 2.0490624 | 1.5937152 | 2.0490624 |

Nanotechnology Perceptions Vol. 20 No.S1 (2024)

| 30 | 1.15 | 2400.3375 | 2.16030375 | 1.68023625 | 2.16030375 |
|----|------|-----------|------------|------------|------------|
| 50 | 1.2 | 2613.6 | 2.35224 | 1.82952 | 2.35224 |

In STAAD Pro, the wind load is calculated using the data that was just mentioned. Table No. 18 of IS 875 (Part 3) 2015 is used to compute the external pressure co-efficient (Cpe) for curved roofs based on clause 7.3.3.6. For H/L = 0.5, the wind-ward and lee-ward factors are 1.2 and 0.7, respectively.

5.4 Seismic load

IS 1893:2016 was used to calculate the seismic load on the structure. Below is a list of the seismic parameters taken into account.

| Values |
|--------|
| 0.36 |
| 5.00 |
| 1.5 |
| 2.00 |
| 3 |
| 2 % |
| |

VI. RESULTS AND OBSERVATION

C1 and CII = Class I & Class II

M1 and M2 = Method1 & Method II

A. Maximum node displacement for class I and class II subdivision

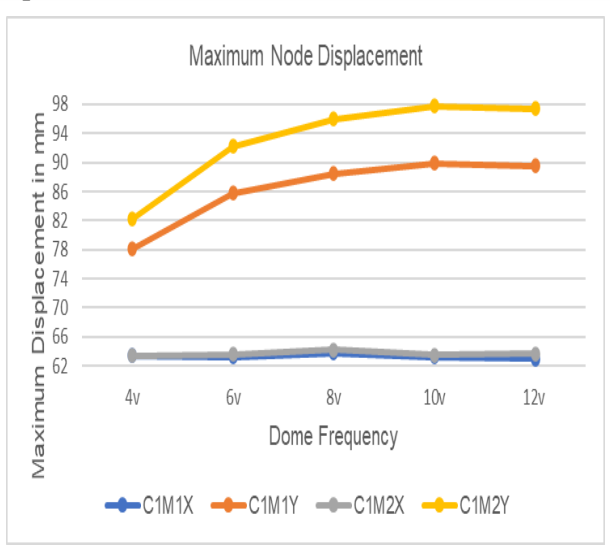


Figure 9 Maximum node displacement for Class I breakdown method I & II

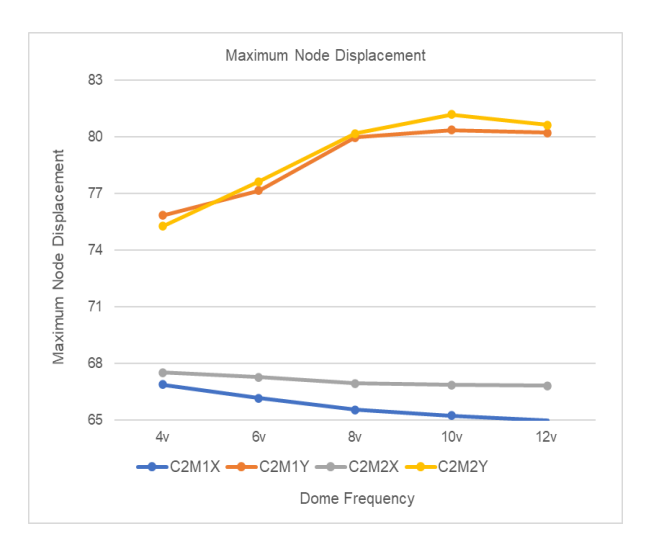


Figure 10 Maximum node displacement for Class I breakdown method I & II

It has been found that the maximum node displacement increases as dome frequency increases for both the breakdown methods, method 1 and method 2, for both the subdivisions, class I and class II, from 4v to 10v. If we increase dome frequency even further, the maximum node displacement for Y-direction decreases. But in X-direction for both the breakdown methods 1 and 2 and for both the subdivisions i.e. for class I and class II the maximum node displacement reduces as an increase in dome frequency.

B. Maximum beam displacement

Maximum beam displacement is observed in the bottom section of the dome. In beam displacement, as we increase the dome frequency displacement is reduced.

C. Base shear

Base shear increases an increase in dome frequency, dome radius, and for Class I & II for methods 1 and 2.

D. Maximum shear force

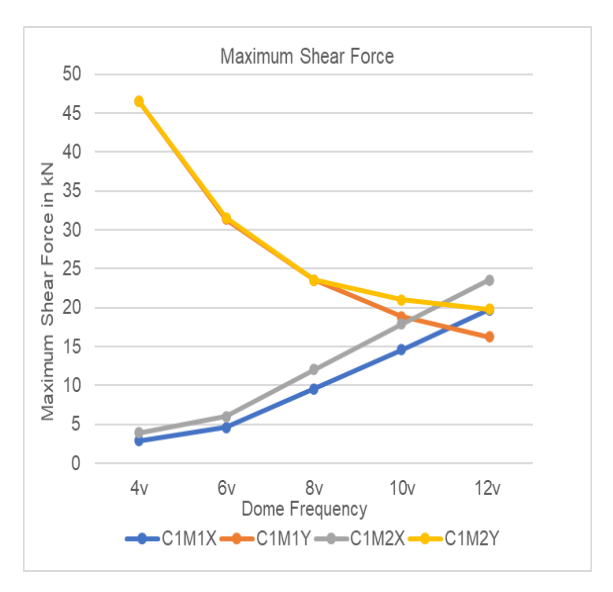


Figure 11 Maximum shear force for Class I breakdown method I & II

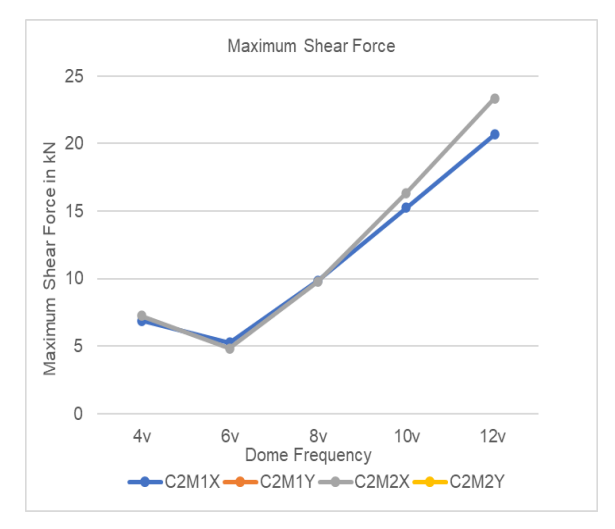


Figure 12 Maximum shear force for Class II breakdown method I & II

Shear force in Y-direction for breakdown method 1 and 2 of both the classes i.e. for class I and class II subdivisions decreases as increase in dome frequency whereas for breakdown method 1 and 2 of class I subdivision the shear force in Z-direction increases as increase in dome frequency but for breakdown method 1 and 2 of class II subdivision the shear force in Z-direction decreases from 4v to 6v further increase in dome frequency the maximum shear force also increases in Z-direction.

E. Maximum bending moment

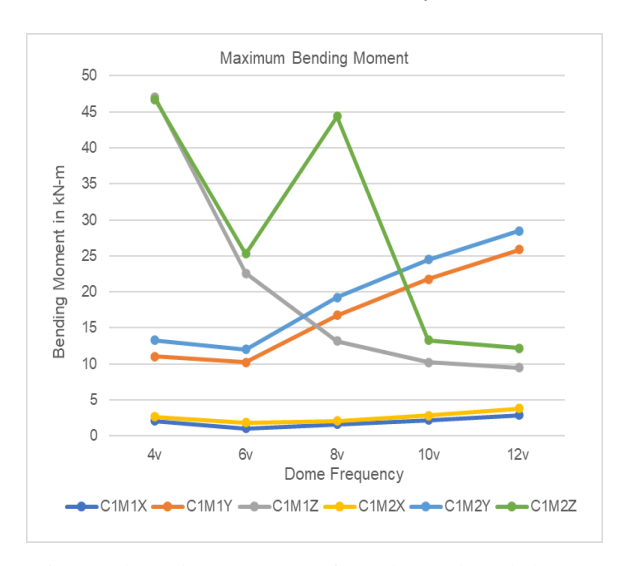


Figure 13 Maximum bending moment for Class I breakdown method I & II

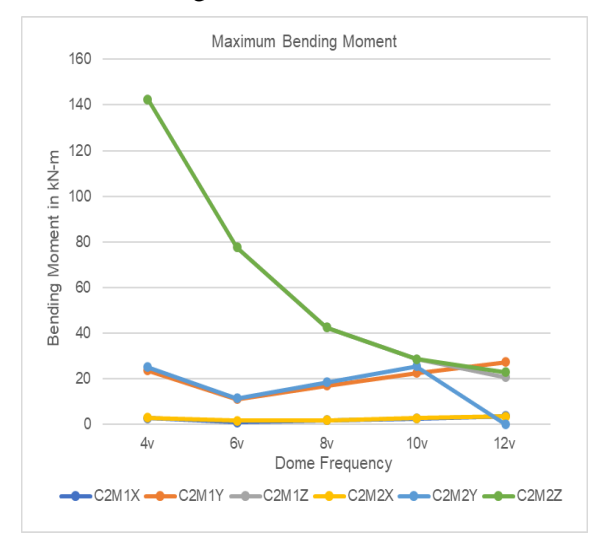


Figure 14 Maximum bending moment for Class I breakdown method I & II

Bending moment in Y-direction for breakdown method 1 and method 2 of class I and for breakdown method 1 of class II subdivision, increases in dome frequency from 4v to 6v will lead to decrease in bending moment again further increase in dome frequency will lead to increase in bending moment in Y-direction, whereas, in breakdown method 2 of class II subdivision. The bending moment in Y-direction decreases as increase in frequency from 4v to 6v, further increase in dome frequency will lead to increase in bending moment from 6v to 10v but again we increase dome frequency from 10v to 12v the maximum bending moment in Y-direction will gets reduced.

F. Reaction at support

Nanotechnology Perceptions Vol. 20 No.S1 (2024)

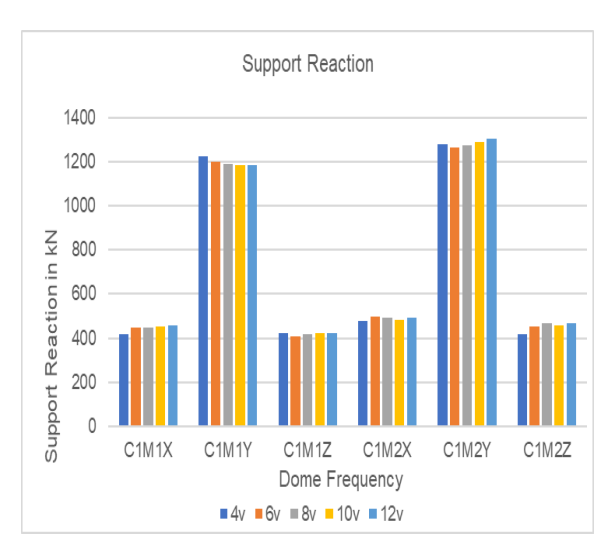


Figure 15 Maximum support reaction for Class I breakdown method I & II

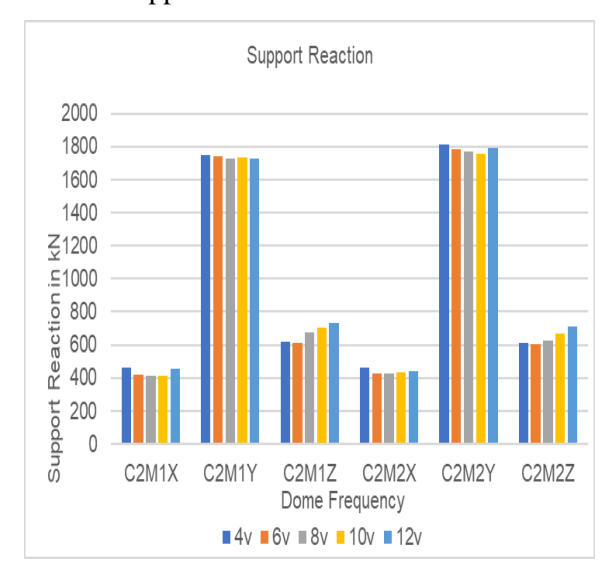


Figure 16 Maximum support reaction for Class II breakdown method I & II

Maximum reaction at support in Y-direction for breakdown method 1 and 2 of both the classes i.e. for class I and class II subdivisions decrease as an increase in dome frequency.

G. Moment at support

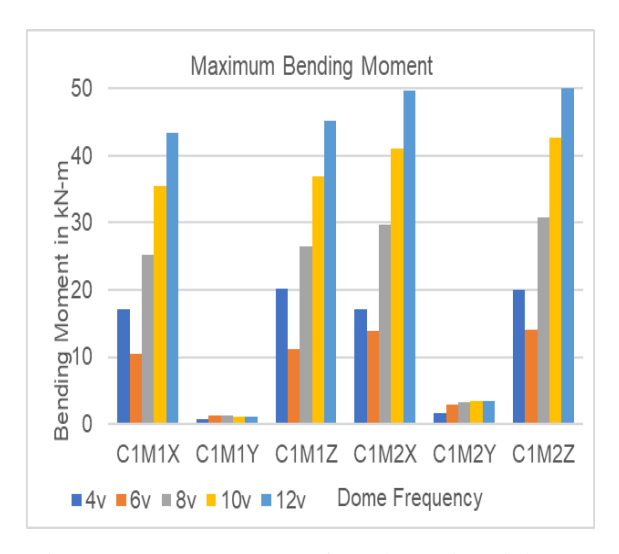


Figure 17 Maximum support moment for Class I breakdown method I & II

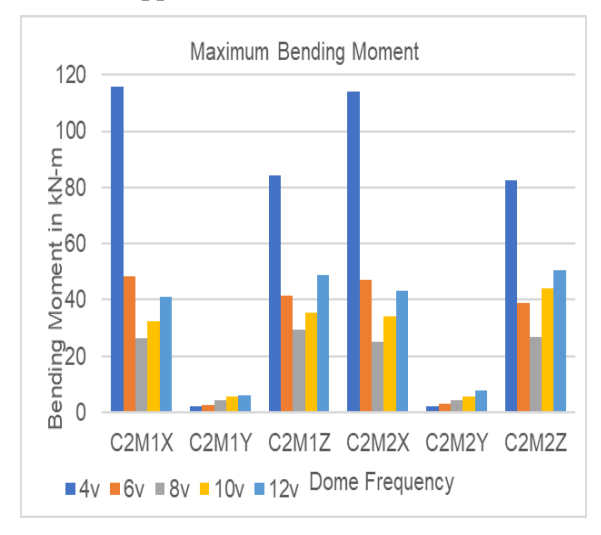


Figure 18 Maximum support moment for Class II breakdown method I & II

The maximum moment at support in the Y-direction for breakdown method 1 of class I subdivision increases from 4v to 8v further increase in frequency will lead to a decrease in moment in Y-direction but for breakdown method 2 of class I and for breakdown method 1 and 2 of class II subdivisions the maximum moment increases as increase in dome frequency.

H. Axial force

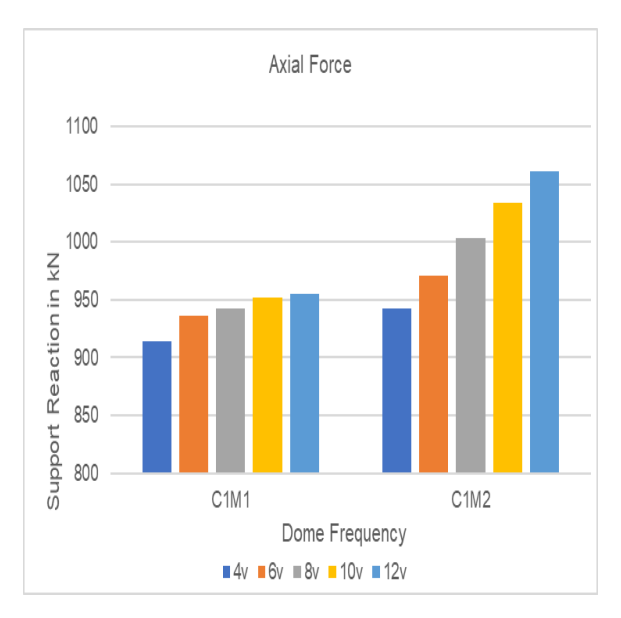


Figure 19 Maximum axial force for Class I breakdown method I & II

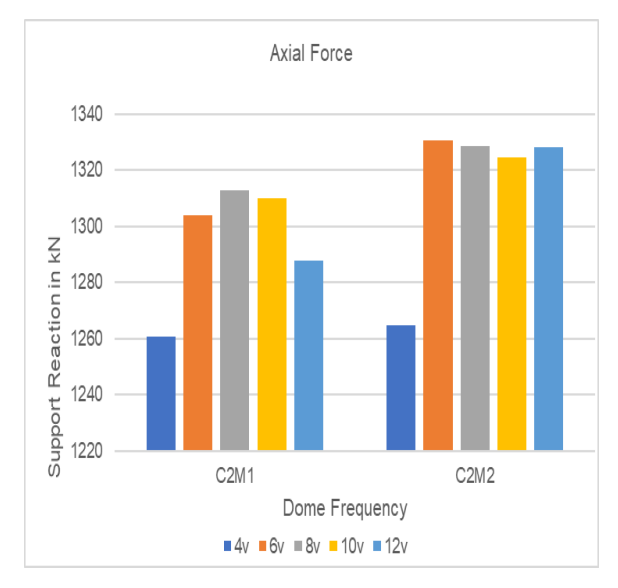


Figure 20 Maximum axial force for Class II breakdown method I & II

According to the aforementioned graphs, it can be seen that the maximum axial force for the breakdown method 1 and method 2 of class I subdivision increases as an increase in dome frequency. For breakdown method 1 of class II subdivision the maximum axial force increases as an increase in frequency from 4v to 8v again increase in dome frequency will give a decrease in axial force whereas, in breakdown method 2 of class II subdivision the maximum axial force increases as an increase in frequency from 4v to 8v but again in 10v the axial force decreases but further increase in frequency will lead to increase in axial force.

Nanotechnology Perceptions Vol. 20 No.S1 (2024)

VII. CONCLUSION

For both classes I and II, as well as for both the breakdown techniques i.e. techniques 1 and 2, the structure's weight increases as the dome frequency rises. Maximum nodal displacement is observed at the top for both class I & II and the breakdown method for all dome frequencies. It has been noted that displacement decreases as dome frequency increases. In comparison to 6v, 8v, 10v, and 12v, dome frequency 4v shows the largest beam displacement. Maximum beam displacement was seen at the top of the dome for 4v & 6v dome frequency for the breakdown method (i.e. Method 1 & Method 2) of class I.

Due to class I's shorter strut length, there are more beams observed in class I than in class II. Base shear (VB) is increasing as dome frequency increases for both class I & II and the breakdown method. Maximum axial force for method 1 of class I is increasing as dome frequency increases whereas, for breakdown method 1 of class II, it increases till 8v & decreases for 10v & 12v by 0.23% & 1.69% respectively. For method 2 of class I the maximum axial force increases as an increase in dome frequency whereas, for method 2 of class II it increases from 4v to 6v & decreases in 8v & 10v by 0.16% & 0.46% respectively compared with 6v & again it increases in 12v by 0.27% compared with 10v. The maximum support reaction for method 1 of class I is reducing as dome frequency increases however, for class II for breakdown method 1 it is reducing from 4v to 8v & in 10v it is increased by 0.74% & 0.51% respectively & again it is reduced in 12v by 0.2% & 0.3% respectively. For breakdown method 2 of class I the maximum support reaction is reduced from 4v to 6v after 6v both increasing with an increase in dome frequency. The reduction percentage for support reaction in the Y-direction is 0.922%, while for class II subdivision for the breakdown method 2, support reaction is reducing as dome frequency increases till 10v & in 12v it increased by 7.12% & 1.82% respectively.

The maximum support moment for method 1 & method 2 of class I is reduced from 4v to 6v & after the 6v moment increases as dome frequency increases. The reduction percentage for method 1 in the x-direction is 39.083% & for the z-direction is 44.72% & for method 2 in the x-direction is 19.27% & for the z-direction is 29.50%. For method 1 & method 2 of the class II subdivision, the maximum support moment is reduced from 4v to 8v & from 10v onwards moment increases as dome frequency increases. The increased percentage for method 1 is 23.68% in the x-direction & 20% in the z-direction & for method 2 it is increased by 36.04% in the x-direction & 66.26% in the z-direction. Breakdown method 1 & method 2 of class I maximum shear force is reduced as dome frequency increases while, for method 1 & method 2 of class I maximum bending moment is reduced from 4v to 6v & on 8v onwards it increases as dome frequency increases. The increased percentage in 8v for method 1 is 63.65% & for method 2 is 60.09%.

Maximum shear force for breakdown method 1 & method 2 of class II is reducing as dome frequency increases although, for method 1 & method 2 of class II maximum bending moment is reducing from 4v to 6v & from 8v onwards it goes on increasing as dome frequency increases. The increased percentage in 8v for method 1 is 52.26% & for method 2 is 63.04%.

References

- [1] Mandali D. G, Ramani S. D, May 2016, "Comparative Study for Geodesic Dome of Class I Subdivisions" Journal of Emerging Technologies and Innovative Research (JETIR), Volume 3, Issue 05, ISSN: 2349-5162, pp. 165-171.
- [2] Lakhov A. Ya., March 2017, "Logical Classification of Geodesic Shells and Domes" ARPN Journal of Engineering and Applied Sciences, Volume 12, Issue 05, ISSN: 1819-6608, pp. 1547-1553.
- [3] Shrivastava A, Pendharkar U (2021), "Study of Optimized Sectional Shape for Geodesic Domes" Journal of Xi'an University of Architecture & Technology, Volume 13, Issue 01, ISSN: 1006-7930, pp. 407-411.
- [4] Ghugare V. G, Prof. Sapate V, April 2021, "Structural Analysis of Dome Structure by STAAD Pro" International Journal for Research in Applied Science & Engineering Technology (IJRASET), Volume 9 Issue 4, ISSN: 2321-9653, pp. 1515-1520.
- [5] Kunjan Bharwad, Satyen Ramani, "Structural Optimization of Class2(Method2) Type Geodesic Steel Dome Using ANSYS® Workbench", Journal of Emerging Technologies and Innovative Research (JETIR), Volume 4, Issue 04, ISSN-2349-5162, April 2017, pp. 341-349.
- [6] Ansa T Varghese, Manju George, "Study on the effect of Diameter, Compressive Strength and Number of Ribs on the Large Concrete Monolithic Dome" International Journal of Engineering Development and Research (IJEDR), Volume 3, Issue 4, ISSN: 2321-9939, 2015, pp. 300-303.
- [7] Riya Anna Abraham, G. Kesava Chandran, "Study of Dome structures with specific Focus on Monolithic and Geodesic Domes for Housing" International Journal of Emerging Technology and Advanced Engineering (IJETAE), Volume 6, Issue 08, ISSN: 2250-2459, August 2016, pp. 173-182.
- [8] IS 1893 (Part 4): 2005, Indian standard criteria for earthquake-resistant design of structures (Part 4 Industrial structures including stack-like structures). Bureau of Indian Standards, New Delhi.